8th U. S. National Combustion Meeting
Organized by the Western States Section of the Combustion Institute
and hosted by the University of Utah
May 19-22, 2013

Predictive Theoretical Kinetics of the Pressure-Dependent Spin-Forbidden Reaction O + CO → CO_2

Ahren W. Jasper[1] and Richard Dawes[2]

[1]Combustion Research Facility, Sandia National Laboratories, Livermore, CA 94551, USA
[2]Missouri University of Science and Technology, Rolla, MO 65401, USA

The kinetics of the spin-forbidden reaction CO + O → CO_2 is fully characterized theoretically. Global analytic representations of the lowest-energy singlet surface, the two lowest-energy triplet surfaces, and their spin–orbit coupling surfaces are obtained via dynamic weighted multireference electronic structure theory calculations and the interpolated moving least squares (IMLS) semiautomated surface fitting strategy. The analytic spin–orbit-coupled representation is used in full-dimensional electronically nonadiabatic molecular dynamics calculations, where the spin-forbidden dynamics is modeled using the coherent switches with decay of mixing (CSDM) multistate trajectory method. The trajectory calculations reveal direct (nonstatistical) and indirect (statistical) spin-forbidden reaction mechanisms. The resulting high pressure limit rate coefficient is more than an order of magnitude larger than the calculated value used in many detailed models of combustion and is larger than an application of "nonadiabatic transition state theory" (NA TST). This discrepancy is attributed to nonstatistical and multidimensional effects not present in the NA TST model. Pressure dependence is characterized via trajectory ensembles of CO_2 + Kr collisions, which are used to parameterize a detailed model of energy transfer. In most kinetics applications where collisional energy transfer information is needed, it is estimated or determined empirically whereas here it is predicted without empiricism. The resulting energy transfer model is used to calculate the low-pressure limit rate coefficient, which is found to be ~3x larger than available experimental values at 3000–4600 K. Together, these calculations provide a complete first-principles (parameter-free) characterization of the kinetics of this system, which is particularly challenging as it involves spin-forbidden dynamics and pressure dependence.

1. Introduction

The spin-forbidden oxidation of CO to CO_2 by ground-state (triplet) atomic oxygen O

$$O + CO\ (+M) \longrightarrow CO_2\ (+M) \tag{1}$$

has been identified as important in some combustion systems (particularly at high pressures), where it competes with the oxidation of CO by OH, N_2O, etc [1]. Few theoretical studies of the spin-forbidden kinetics or dynamics of this system have appeared previously. Troe [2] calculated the high-pressure association rate coefficient ($k_{1\infty}$), and Westmoreland et al. [3] fit experimental falloff kinetics to the results of QRRK calculations. These expressions (with some adjustments [1]) are used in many detailed chemical models of combustion [4,5].

The relevant potential energy surfaces have been studied previously. Hwang and Mebel [6] characterized the energetics of the lowest-energy singlet and lowest-energy triplet surfaces of CO_2 using several levels of electronic structure theory. They identified two spin-forbidden mechanisms for the oxidation of CO by O: a "direct" mechanism via a singlet-triplet curve crossing associated with a collinear geometry and an extended incipient C–O bond distance

$$O + CO \sim\!> CO_2\ \text{(direct)}, \tag{1'}$$

("$\sim\!>$" denotes a spin-forbidden event) and an "indirect" mechanism where a short-lived triplet complex $^3CO_2$ is formed and quenched via a singlet-triplet curve crossing associated with a bent geometry, i.e.,

$$O + CO \rightleftarrows {}^3CO_2 \sim\!> CO_2\ \text{(indirect)}. \tag{1''}$$

Based on the energetics and spin-orbit coupling strengths calculated at the linear and bent crossing seams, both mechanisms were suggested to be important. In other work, analytic potential energy surfaces for the three lowest triplet states of CO_2 based on multireference perturbation theory calculations were developed and used in adiabatic (i.e., uncoupled, single state) classical trajectory hyperthermal scattering calculations [7,8] with favorable comparisons with

experimental results. These two sets of theoretical studies did not include any spin-forbidden or pressure dependent kinetics or dynamics.

Experimental kinetics studies of the thermal decomposition of CO_2 (reaction –1) have been carried out at high temperatures and low pressures [9,10,11]. Under these conditions, the CO_2 decomposition reaction is close to 2nd order (i.e., reaction –1 is near the low-pressure CO_2 + M limit), and in this limit the unimolecular decomposition rates are determined by the rates of collisional energy transfer [12,13] and not by the spin-forbidden dynamics. There has been some experimental work at elevated pressures, with decomposition studied at pressures as high as 300 atm [14,15] and association measured up to 24 atm [16]. In both of these studies, extrapolations to higher pressures resulted in limiting values consistent with Troe's value of $k_{1\infty}$. However, even at the highest pressures experimentally probed, the reaction was observed to close to a second order (low-pressure-limit) picture. We are not aware of any experimental studies that have directly probed the high-pressure limit spin-forbidden kinetics of reaction 1 in either the forward or reverse direction.

Here we present an electronic structure study of the lowest-energy singlet and the two lowest-energy triplet surfaces, a spin-forbidden molecular dynamics study to predict the high-pressure limit of reaction 1, and a collisional energy transfer molecular dynamics study to predict the low-pressure l limit of reaction 1.

2. Theory

Quantum Chemistry and Analytic Potential Energy Surfaces. Reaction 1 proceeds initially on one of three triplet surfaces, and the formation of stable CO_2 requires a spin-forbidden transition to the ground state singlet surface. The lowest-energy singlet (^{1}A' or S) and the two lowest-energy triplet (^{3}A' or T1 and ^{3}A" or T2) surfaces were characterized at the dw-MRCI+Q/CBS level of theory, where: three triplet and five singlet states were dynamically weighted (dw) in the CASSCF step with a weighting range parameter of β = 4.5 eV, the Davidson correction (+Q) was applied to the multireference configuration interaction (MRCI) energies, the complete basis set CBS limit was extrapolated using a two-point l^{-3} formula and the aug-cc-pVTZ and aug-cc-pVQZ basis sets, and an active space of 12 electrons in 10 orbitals (12e,10o) was used, corresponding to a nearly full valence active space with two additional occupied orbitals excluded. The third nonreactive triplet surface is not considered here.

Spin–orbit coupling surfaces were calculated using: the Breit-Pauli Hamiltonian ($\hat{H}_{SO}$) as implemented in the electronic structure program Molpro, the dw-CASSCF/aug-cc-pVQZ method, and the (12e,10o) active space. The two geometry-dependent spin–orbit coupling surfaces are defined

$$\varepsilon_1 = \left| \left\langle {}^1A' \middle| \hat{H}_{SO} \middle| {}^3A' \right\rangle \right| \tag{2a}$$

$$\varepsilon_2 = \left| \left\langle {}^1A' \middle| \hat{H}_{SO} \middle| {}^3A'' \right\rangle \right|, \tag{2b}$$

where the triplet wave functions are a sum over three triplet spin-states. These quantum chemistry methods are expected to be spectroscopically accurate for a small system like CO_2, such that the contribution to the overall error in the dynamics and kinetics calculations discussed below arising from the potential energy surfaces (PESs) may be assumed to be negligible.

An analytic global representation of the 3 x 3 diabatic potential energy matrix

$$\mathbf{U} = \begin{pmatrix} V_S & \varepsilon_1 & \varepsilon_2 \\ \varepsilon_1 & V_{T1} & 0 \\ \varepsilon_2 & 0 & V_{T2} \end{pmatrix} \tag{3}$$

where V_X is the PES of state X (X = S, T1, or T2), was obtained by fitting the results of the ab initio methods discussed above using the IMLS semiautomatic fitting method [17]. The resulting analytic surfaces very accurately fit the multireference quantum chemistry data, with a root-mean-squared fitting error of only 0.02 kcal/mol.

Nonadiabatic Molecular Dynamics and High Pressure Kinetics. The high pressure limit of reaction 1 was calculated via coupled-states molecular dynamics. Specifically, the coherent switches with decay of mixing (CSDM) multistate trajectory method [18] was used. CSDM trajectories propagate on a mean-field potential energy surface, which is a weighted average of the diabatic potential energy surfaces. The mean-field weights are given by the electronic state populations, which are obtained by integrating the solution to the time-dependent electronic Schrödinger equation along each CSDM trajectory. Electronic decoherence [19] is explicitly included via de-mixing terms. De-mixing forces each CSDM trajectory into a quantized electronic state in the absence of coupling. The CSDM method may be thought of as

intermediate of the more widely employed surface hopping method and of mean field methods. Like surface hopping trajectories, CSDM trajectories are electronically quantized away from regions of coupling and therefore share the desirable features of being able to explore low-probability events, having physical internal energy distributions, etc. Unlike surface hopping trajectories, however, CSDM trajectories do not feature sudden momentum changes and the associated problem of frustrated hops, and the results of CSDM trajectories are dependent on the choice of electronic representation. CSDM trajectories also include an explicit treatment of electronic decoherence. The CSDM method was shown to be the most accurate of several multistate trajectory methods in tests against quantum mechanical results for atom–diatom scattering reactions and featuring several different couplings types and strengths [20].

The initial rovibrational state of CO was selected *classically* from a thermal distribution at temperature T by sampling the initial coordinates and momenta evenly in time from isolated CO trajectories subject to an Andersen thermostat. The impact parameter b was selected evenly in b^2 from 0– $b_{\max}^2$ ($b_{\max}$ = 2 Å), with the relative collision energy selected from a thermal distribution and an initial O–CO center-of-mass distance of 4 Å. We confirmed that these sampling limits were suitable for the temperatures considered here.

Product channels were assigned to each trajectory by monitoring the two C–O distances and the electronic state populations. Bimolecular products were identified when one C–O bond distance exceeded 4 Å, and the molecular product CO_2 was identified when the incipient bond distance was shorter than 1.3 Å and the instantaneous electronic state population for the singlet was greater than 0.99. Using standard formulas, the reaction cross section is

$$\sigma_\alpha^s(T) = \pi b_{\max}^2 F_\alpha^s(T)\,, \tag{4}$$

where s = T1 or T2 and labels the initial electronic state, α labels the products, and F_α^s is the fraction of trajectories that finish the trajectory simulation in the α product channel. The related rate coefficients are

$$k_\alpha^s(T) = g_e \sqrt{\frac{8k_BT}{\pi\mu}}\sigma_\alpha^s\,, \tag{5}$$

where μ is the reduced mass of CO and O, and g_e is the ratio of the electronic partition functions for the reactive surfaces and reactants (3/9). One-sigma uncertainties were calculated in the usual way for binned quantities. The total rate coefficient includes contributions from both reactive triplet states:

$$k_\alpha(T) = k_\alpha^{T1} + k_\alpha^{T2}\,, \tag{6}$$

where $k_{1\infty}(T) \equiv k_S(T)$ with α = S for the singlet CO_2 product.

Collisional Energy Transfer Molecular Dynamics and Low Pressure Kinetics. The weakest link in many theoretical chemical kinetics applications is the treatment of collisional energy transfer, which gives rise to pressure dependence. Here, we have used CO_2 + Kr trajectory ensembles to calculate low-order moments of the total energy E and total angular momentum J transferred due to the collisions [21,22]. As we are principally interested in low-order moments, we may expect the classical approximation used here to be a good one. The dominant source of uncertainty in these calculations instead likely arises from the choice of the potential energy surface. We used the singlet CO_2 PES discussed above with additional "exp/6" CO_2–Kr terms obtained by fitting CO_2–Kr counterpoise-corrected CCSD(T)/CBS interaction energies. The good accuracy of this so-called "separable pairwise" approximation for the PES has been previously validated for energy transfer studies involving atomic baths [22].

The calculated low-order moments were used to parameterize simple models of collisional energy transfer. The simplest model considered here is the well-known single-exponential-down model, which has a single parameter $\alpha = \langle\Delta E_d\rangle$, where $\langle\Delta E_d\rangle$ is the average energy transferred in deactivating collisions and the activating wing is determined via detailed balance. We also consider a two-dimensional model for collisions, i.e., a model that is explicitly a function of both ΔE *and* ΔJ. Specifically, we consider a simple example of such a model, where the probability that a collision knocks the system from some internal state (E,J) to some other state (E',J') is given by

$$P(E,J;E',J') = C\exp(-|\Delta E|/\alpha)\exp(-|\Delta J|/\gamma) \qquad \text{for } \Delta E < 0 \text{ and } \Delta J < 0 \tag{7}$$

with $\Delta E = E - E'$, $\Delta J = J - J'$. C normalizes and enforces detailed balance in P.

Equation 7 may be used directly in two-dimensional versions of the master equation. Here, we calculate the low-pressure limit of reaction 1 using eq 7 as follows. For single-well processes, the low-pressure limit rate coefficient can be written [12,13]

$$k_{1,0} = Z\sum_{J'}\int_{0}^{E_J'} dE'h(E',J')f(E',J')\sum_{J}\int_{E_J}^{\infty} dE'P(E,J;E',J') \tag{8}$$

where the J-dependent thresholds are denoted E_J. Rearrangement of the single-well/single-channel master equation gives coupled equations for the steady-state solutions

$$h(E,J) = \frac{\sum_{J'}\int_{0}^{\infty} dE'\,Z\,P(E',J';E,J)h(E',J')}{Z - k^{0}_{T,p}} \quad \text{for } E < E_J \tag{9}$$

$$h(E,J) = 0 \quad \text{for} \quad E > E_J \tag{9'}$$

where $h = x/f$, f are the Boltzmann populations, and x are the steady-state solutions. Equation 9' enforces the low-pressure condition. Generally, $Z >> k_{1,0}$, and so we can write eq 9 as

$$\mathbf{h} = \mathbf{P}\cdot\mathbf{h}\,, \tag{10}$$

where **h** is a column vector of all the nonzero elements of $h(E,J)$, and **P** is a matrix representation of P with the same ordering. Equation 10 can be solved via linear algebra or via iteration, and resulting **h** may be used to calculate $k_{1,0}$ from eq 8.

3. Results and Discussion

The results of the CSDM calculations for $k_{1\infty}(T)$ for T = 2000–5000 K are shown in Fig. 1 and can be expressed

$$k_S^{T1}(T) = 6.1\times10^{-13}\exp(-1200\ K/T)\ \text{cm}^3\ \text{molecule}^{-1}\ \text{s}^{-1} \tag{11}$$

$$k_S^{T2}(T) = 8.0\times10^{-13}\exp(-5500\ K/T)\ \text{cm}^3\ \text{molecule}^{-1}\ \text{s}^{-1} \tag{12}$$

$$k_{1\infty}(T) = 1.1\times10^{-12}\exp(-2000\ K/T)\ \text{cm}^3\ \text{molecule}^{-1}\ \text{s}^{-1}\ . \tag{13}$$

The present value of $k_{1\infty}(T)$ is 24–32x larger than the existing theoretical literature value for the high pressure limit of reaction 1 [2]. Both reactive triplet states contribute significantly to the total rate for reaction 1. Despite the similar singlet-triplet coupling strengths for the two triplet surfaces, k_S^{T1}/k_S^{T2} = 4 at 1000 K and 1.4 at 5000 K. The differing values of k_S^{T1} and k_S^{T1} and their different temperature dependence can be largely attributed to their different spin-forbidden reaction thresholds.

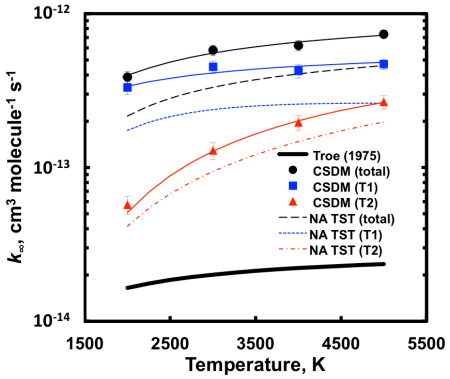

Figure 1. High pressure limit rate coefficient for reaction 1 calculated using the CSDM method (symbols and solid lines), calculated using NA TST (dashed lines), and from Ref. 2 (thick solid line).

Also shown in Fig. 1 are the results of an application of the so-called nonadiabatic transition state theory (NA TST) of Morokuma and co-workers [23] and Harvey and co-workers [24] using the analytic PESs discussed above. This application is much simpler than the CSDM calculations, employing harmonic state counts for the seam and the "two-pass" Landau-Zener nonadiabatic transition probability. The total NA TST rate coefficient is 13–20x larger than the existing literature value [2] and is a factor of ~2 smaller than the CSDM result. The difference in NA TST and CSDM values can be attributed to the neglect of multidimensional effects in NA TST [25].

We have further analyzed the multistate trajectory calculations to reveal the following dynamical details. The reaction proceeds initially with equal populations on the two triplet surfaces (and a third nonreactive triplet surface that is not considered here). On either reactive surface, the system first encounters an electronically adiabatic transition state associated with a triplet saddle point and an incipient bond distance of R = 1.9 Å. These dynamical bottlenecks focus the system with respect to the O–C–O bond angle θ, such that the system will likely first encounter the subsequent crossing seam with bond angles close to that of the saddle points (120°). At the crossing seams, there is some small probability for switching to the singlet surface, and a successful surface switch quickly leads to the formation of singlet CO_2. The system is more likely, however, to stay on the triplet surface and to encounter the shallow $^3CO_2$ well. These features are not deep enough to significantly trap the system, but they may delay the system and promote multiple seam crossings. If the $^3CO_2$ species are long lived enough, one might expect a statistical distribution of seam crossings. We may identify the following direct and indirect spin-forbidden reaction mechanisms: The "direct" spin-forbidden mechanism is associated with the first set of seam crossings and features a nonstatistical distribution at the crossing seam shaped by the preceding saddle point. The "indirect" spin-forbidden mechanism, on the other hand, is the result of sufficient equilibration in the $^3CO_2$ wells and features a statistical distribution at the crossing seam. These mechanisms are in the spirit of the direct and indirect mechanisms suggested earlier [6], although unlike Hwang and Mebel we associate the two mechanisms with distinct dynamical effects and not with distinct local minima on the crossing seams.

The collisional energy transfer trajectory ensembles discussed above were used to calculate several low-order energy transfer moments. Here we focus on the first-order moments of ΔE and ΔJ for deactivating collisions only. The results may be summarized for M = Kr and 1000–5000 K as

$$< \Delta E_d >= 185\ (T / 300\,\mathrm{K})^{0.85}\ \mathrm{cm}^{-1}, \tag{14}$$

$$< \Delta J_d >= 8.8\ (T / 300\,\mathrm{K})^{0.45}\ \hbar, \tag{15}$$

where the moments have been scaled to a Lennard-Jones collision frequency calculated using trajectory-based parameters: σ = 3.92 Å, ε = 144 cm^{-1}. The low pressure limit of reaction 1 calculated using the two-dimensional energy transfer model in eq 7, $\alpha = <\Delta E_d>$, and $\gamma = <\Delta J_d>$ is ~70% smaller than the low pressure limit calculated with the widely-used one-dimensional single exponential down model with $\alpha = <\Delta E_d>$.

Pressure-dependent kinetics was calculated by solving the master equation and using the detailed high-pressure and low-pressure kinetics information discussed above. The present predicted values are compared with the high temperature (3000–4600 K) experimental results of Wagner and Zabel [15] in Fig. 2 for pressures from 5–320 atm. The present values are 2.5–3.5x larger than the experimental values at the lowest pressures accessed in the Wagner and Zabel experiments. At these pressures (~6 atm), the calculations show very little deviation from the low-pressure limiting result, k_0[M]. At the higher range of experimental pressures, and the calculations show some deviation from k_0[M] (by up to ~40%). The experimental results show a similar (but somewhat more significant) effect.

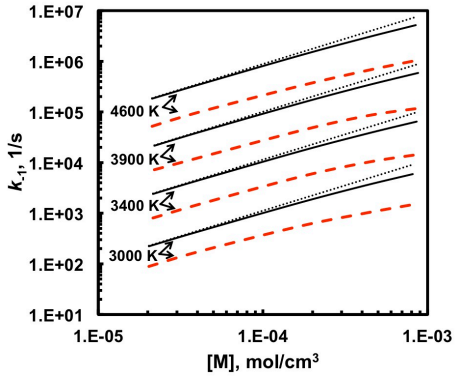

Figure 2. High temperature, low pressure rate coefficients for CO_2 decomposition (reaction –1). The calculated values are shown as thin solid black lines. The calculated low-pressure-limits, k_0[M], are shown as thin dotted black lines. The experimental values of Wagner and Zabel [15] are represented by the thick red dashed lines.

4. Conclusions

A complete first principles theoretical characterization of the reaction O + CO was presented. This characterization included high-level multireference quantum chemistry calculations, multistate trajectory calculations for the high-pressure-limit spin-forbidden kinetics, and collisional energy transfer trajectory calculations for the low-pressure-limit

kinetics. The high-pressure limit predicted here is more than an order of magnitude larger than an earlier calculation. The high-temperature low-pressure kinetics were found to be ~3x larger than the experimental results of Wagner and Zabel. The effect that changes to this rate coefficient have on the predictions of detailed models of combustion is currently being investigated [26].

Acknowledgement

This work is supported by the Division of Chemical Sciences, Geosciences, and Biosciences, Office of Basic Energy Sciences, U.S. Department of Energy (Contract No. DE-AC04-94-AL85000).

References

[1] M. T. Allen, R. A. Yetter, and F. L. Dryer, *Combus. Flame* **109**, 449 (1997).
[2] J. Troe, *Fifteenth Symp. (Int.) Combust.* **15**, 667 (1975).
[3] P. R. Westmoreland, J. B. Howard, J. P. Longwell, and A. M. Dean, *AIChE J.* **32**, 1971 (1986).
[4] S. G. Davis, A. V. Joshi, H. Wang, and F. Egolfopoulos, *Proc. Combust. Inst.* **30**, 1283 (2005).
[5] A. M. Starik, N. S. Titova, A. S. Sharipov, and V. E. Kozlov, *Combust. Explosion Shock Waves* **46**, 491 (2010).
[6] D.-Y. Hwang and A. M. Mebel, *Chem. Phys.* **256**, 169 (2000).
[7] M. Braunstein and J. W. Duff, *J. Chem. Phys.* **112**, 2736 (2000).
[8] A. L. Brunsvold, H. P. Upadhyaya, J. Zhang, R. Cooper, T. K. Minton, M. Braunstein, and J. W. Duff, *J. Phys. Chem. A* **112**, 2192 (2008).
[9] M. A. Oehlschlaeger, D. F. Davidson, J. B. Jeffries, and R. K. Hanson, *Z. Phys. Chem.* **219**, 93 (2005).
[10] S. Saxena, J. H. Kiefer, and R. S. Tranter, *J. Phys. Chem. A* **111**, 3884 (2007).
[11] Numerous earlier experimental studies exist; see, e.g., Ref. 10 for a critical review of existing experimental results.
[12] J. Troe, *J. Chem. Phys.* **66**, 4745 (1977).
[13] J. Troe, *J. Chem. Phys.* **66**, 4758 (1977).
[14] W. A. Hardy, H. Vasatko, H. Gg. Wagner, and F. Zabel, *Ber. Busen-Ges. Phys. Chem.* **78**, 76 (1974).
[15] H. Gg. Wagner, and F. Zabel, *Ber. Bunsen-Ges. Phys. Chem.* **78**, 705 (1974).
[16] A. P. Zuev and A. Y. Starikovskii, *Khimicheskaya Fizika*, **11**, 1518 (1992).
[17] R. Dawes, A. F. Wagner, and D. L. Thompson, *J. Phys. Chem. A* **113**, 4709 (2009).
[18] A. W. Jasper, C. Zhu, S. Nangia, and D. G. Truhlar, *Faraday Discuss. Chem. Soc.* **127**, 1 (2004).
[19] O. V. Prezhdo and P. J. Rossky, *J. Chem. Phys.* **107**, 5863 (1997).
[20] A. W. Jasper, S. Nangia, C. Zhu, and D. G. Truhlar, *Acc. Chem. Res.* **39**, 101 (2006).
[21] A. W. Jasper and J. A. Miller, *J. Phys. Chem. A* **113**, 5612 (2009).
[22] A. W. Jasper and J. A. Miller, *J. Phys. Chem. A* **115**, 6438 (2011).
[23] Q. Cui, K. Morokuma, J. M. Bowman, and S. J. Klippenstein, *J. Chem. Phys.* **110**, 9469 (1999).
[24] J. N. Harvey, *Phys. Chem. Chem. Phys*. **9**, 331 (2007).
[25] A. W. Jasper, unpublished (2012).
[26] F. M. Haas, M. Chaos, and F. L. Dryer, private communication (2013).